D-4F decreases brain arteriole inflammation and improves cognitive performance in LDL receptor-null mice on a Western diet

Georgette M. Buga,[1,*] Joy S. Frank,[*] Giuliano A. Mottino,[*] Michael Hendizadeh,[*] Ashkan Hakhamian,[*] Jan H. Tillisch,[*] Srinivasa T. Reddy,[*,†] Mohamad Navab,[*] G. M. Anantharamaiah,[§] Louis J. Ignarro,[†] and Alan M. Fogelman[*]

Departments of Medicine* and Molecular and Medical Pharmacology,[†] David Geffen School of Medicine at the University of California–Los Angeles, Los Angeles, CA 90095-1679; and the Atherosclerosis Research Unit, Department of Medicine,[§] University of Alabama at Birmingham, Birmingham, AL 35294

Abstract LDL receptor-null mice on a Western diet (WD) have inflammation in large arteries and endothelial dysfunction in small arteries, which are improved with the apolipoprotein A-I mimetic D-4F. The role of hyperlipidemia in causing inflammation of very small vessels such as brain arterioles has not previously been studied. A WD caused a marked increase in the percent of brain arterioles with associated macrophages (microglia) ($P < 0.01$), which was reduced by oral D-4F but not by scrambled D-4F (ScD-4F; $P < 0.01$). D-4F (but not ScD-4F) reduced the percent of brain arterioles associated with CCL3/macrophage inflammatory protein-1α ($P < 0.01$) and CCL2/monocyte chemoattractant protein-1 ($P < 0.001$). A WD increased ($P < 0.001$) brain arteriole wall thickness and smooth muscle α-actin, which was reduced by D-4F but not by ScD-4F ($P < 0.0001$). There was no difference in plasma lipid levels, blood pressure, or arteriole lumen diameter with D-4F treatment. Cognitive performance in the T-maze continuous alternation task and in the Morris Water Maze was impaired by a WD and was significantly improved with D-4F but not ScD-4F ($P < 0.05$). We conclude that a WD induces brain arteriole inflammation and cognitive impairment that is ameliorated by oral D-4F without altering plasma lipids, blood pressure, or arteriole lumen size.—Buga, G. M., J. S. Frank, G. A. Mottino, M. Hendizadeh, A. Hakhamian, J. H. Tillisch, S. T. Reddy, M. Navab, G. M. Anantharamaiah, L. J. Ignarro, and A. M. Fogelman. **D-4F decreases brain arteriole inflammation and improves cognitive performance in LDL receptor-null-mice on a Western diet.** ***J. Lipid Res.*** **2006.** 47: **2148–2160.**

Supplementary key words hyperlipidemia • lipoproteins • apolipoprotein A-I mimetic peptides • arterioles • hyperlipidemia • brain function

Feeding a high-fat, high-cholesterol Western diet (WD) to LDL receptor-null ($LDLR^{-/-}$) mice results in accumulation of subendothelial macrophages in large arteries (e.g., aorta) (1, 2) and endothelial dysfunction in small arteries (e.g., facialis artery) associated with arterial wall thickening (3). Oral administration of the apolipoprotein A-I (apoA-I) mimetic peptide D-4F significantly improved these abnormalities (3).

The pathologic effects of hyperlipidemia on small vessels have focused on measurements of vasoreactivity. Ou et al. (3) noted that there was increased wall thickness of the facialis artery after feeding a WD to $LDLR^{-/-}$ mice and that oral D-4F prevented and reversed this thickening. In vitro collagen synthesis was stimulated by oxidized sterols, and this was prevented by treatment with D-4F. Ou et al. (3) implied that the increased collagen synthesis was likely to be responsible in part for the in vivo thickening of the arterial wall.

The accumulation of macrophages in the subendothelial space of large arteries in response to LDL-induced chemokines would be expected, because *i*) LDL is trapped in the subendothelial space and *ii*) a few sentinel macrophages are always present in this space as part of the innate immune system (4–6). The work of Napoli et al. (5) indicates that in large arteries such as the aorta, macrophages are active in the subendothelial space, even in the human fetus.

The facialis artery studied by Ou et al. (3) has a lumen diameter of 180–280 μm, and there is no evidence to suggest that macrophages accumulate in the subendothelial space of such small arteries. Arterioles have lumen diameters of 10 to 100 μm, and there is no evidence of a significant subendothelial space in these small vessels. It is not likely that macrophages could accumulate between the monolayer of luminal endothelial cells and the smooth muscle cell layer that surrounds them without obstructing the lumen.

Manuscript received 15 May 2006 and in revised form 27 June 2006.

Published, JLR Papers in Press, July 12, 2006.
DOI 10.1194/jlr.M600214-JLR200

Abbreviations: $LDLR^{-/-}$, LDL receptor-null; MCP-1, monocyte chemoattractant protein-1; MIP-1α, macrophage inflammatory protein-1α; MWM, Morris Water Maze; ScD-4F, scrambled D-4F; T-CAT, T-maze continuous alternation task; WD, Western diet.

[1] To whom correspondence should be addressed.
e-mail: gbuga@mednet.ucla.edu

Indeed, in arterioles, sentinel macrophages have been shown to reside not in the subendothelial space as in large arteries, but rather on the adventitial side of the vessel (7, 8).

Mouse models suggest that diseases such as Alzheimer's disease may have an inflammatory component similar to atherosclerosis that is associated with very small vessels such as arterioles (9–11). In humans, microvessel-associated monocyte chemoattractant protein-1 (MCP-1) and interleukin-1β were found in Alzheimer's brains but not in non-Alzheimer's brains (12).

The role of hyperlipidemia in causing inflammation of very small vessels such as brain arterioles has not been previously studied. We report here that feeding a WD to LDLR$^{-/-}$ mice induced brain arteriole inflammation and cognitive impairment, which were ameliorated by oral D-4F without altering plasma lipids, blood pressure, or arteriole lumen size.

MATERIALS AND METHODS

Materials

D-4F and scrambled D-4F (ScD-4F; a control peptide with the same D-amino acids but arranged in a sequence that prevents lipid binding, thus rendering the peptide inactive) were synthesized as described (13). All other reagents were from sources previously reported (13).

Mice

Female wild-type and LDLR$^{-/-}$ C57BL/6 mice (Jackson Laboratories, Bar Harbor, ME) were maintained on a chow diet (Ralston Purina) prior to administration of a WD (Teklad/Harlan, Madison, WI; diet No. 88137, 42% fat, 0.15% cholesterol, w/w). The WD was administered to the mice when they were 5–6 weeks old, and the diet was continued for 6–8 weeks. At the time that the WD was started, D-4F or ScD-4F was added to the drinking water at 300 μg/ml and provided ad libitum for 6–8 weeks prior to functional testing and histologic examination. In pilot studies, this period of feeding the WD was found sufficient to produce significant changes in brain arterioles and in cognitive behavior. The mice consumed approximately 2.5 ml of water per day per mouse, and there was no significant difference in water or food consumption between groups. The University of California–Los Angeles Animal Research Committee approved all studies.

Histopathology

For studies of brain arteriole wall thickness, brains were perfusion fixed in 4% paraformaldehyde in phosphate-buffered saline (PBS) at pH 7.4 at physiologic pressures (75–85 mm/Hg for the anesthetized mice) as described by Fernagut et al. (14). Brains were cryopreserved in 10% sucrose in PBS (pH 7.4), embedded in OCT (Tissue-Tek; Miles Laboratories, Ltd., Elkhart, IN), frozen in isopentane at −40°C, and sectioned in a cryostat at −20°C. The frozen brains were coronally cut into 8 μm sections and stained with hematoxylin-eosin (H and E) or immunostained for smooth muscle α-actin (Spring Bioscience, Fremont, CA). Paraffin embedding was also used at the beginning of the study to compare with frozen brain sections. Because comparable results were obtained, both the histological and immunohistochemical studies were performed on frozen sections. Immunohistochemistry for brain macrophage/microglia, CCL3/macrophage inflammatory protein-1α (MIP-1α), and MCP-1 was performed on unperfused freshly removed brains frozen in isopentane at −40°C, rapidly embedded in OCT, and coronally cut into 8 μm sections in a cryostat at −20°C. The following primary antibodies and dilutions were used: rabbit anti-mouse α-actin polyclonal antibody (1:100; Spring Bioscience); rat anti-mouse F4/80 (1:250; Serotec, Raleigh, NC); goat polyclonal anti-MIP-1α (1:25; Santa Cruz Biotechnology, Santa Cruz, CA); and goat polyclonal anti-MCP-1 antibody (1:50; Santa Cruz Biotechnology). The following secondary antibodies and dilutions were used: goat anti-rabbit (1:200, Jackson Immuno Research Labs, Inc., West Grove, PA); goat anti-rat (1:200, Jackson Immuno Research Labs); and donkey anti-goat and donkey anti-rabbit (1:500, Santa Cruz Biotechnology). Vessels were studied in coronal sections from throughout the brain, and all serial sections were used for measurements. Staining for F4/80, MIP-1α, and MCP-1 was performed on serial sections less than 10 μm apart to determine whether the two antibodies localized to the same arteriole. Controls for the immunostaining consisted of sections exposed to secondary-only antibodies in addition to IgG (Sigma-Aldrich, Dallas, TX) and rabbit anti-mouse actin antibody in the case of MCP-1 and F4/80 or to blocking peptide in the case of MIP-1α (Santa Cruz Biotechnology).

Morphometry and associated statistical methods

Measurements of vascular wall thickness were made only on arterioles that were fully distended and perpendicularly cross sectioned. Using a 40× microscope objective, the sectioned vessels were photographed using SPOT Image software. Three measurements of the internal and external diameters were taken for each and were averaged. Vessel sizes were between 10 and 160 μm, and the comparison of wall-to-lumen ratios was made separately for arterioles with internal diameters of 10–20 μm, 21–50 μm, and 51–100 μm. A minimum of 20 arterioles from each group were examined in the cortical area and in the deep white-matter regions from each brain, and the wall thickness and wall-to-lumen ratios were determined. The ratio of immunoreactive wall thickness to the internal diameter of each vessel was determined in sections immunostained for smooth muscle α-actin. All measurements were performed on a single focal plane by one investigator and repeated by two observers blinded to treatment, using an Olympus BH-2 microscope equipped with a 40× lens. The coefficient of variation for interobserver measurements was found to be 14 ± 1%. The total number of brain arterioles and the number of arterioles demonstrating positive F4/80, MIP1-α, or MCP-1 immunostaining were counted to determine the percent of immunolabeling. Twenty microscope fields from each brain were counted at a final magnification of 200× by one investigator and repeated by two observers blinded to treatment. The coefficient of variation for interobserver measurements was found to be 10 ± 1%. All nonvascular cells (those immunopositive for MCP-1 or MIP-1α and those immunonegative) situated within a circle with a diameter of 150 μm around each arteriole were counted at a final magnification of 400×, and the percent of immunopositive cells was determined. Statistical calculations for morphometry were performed using InStat software (Graph Pad, San Diego, CA).

Behavioral studies and associated statistical methods

T-maze continuous alternation task (T-CAT) testing was performed by one investigator unaware of the treatment groups. The T-maze apparatus and the T-CAT procedure were identical to those described by Gerlai et al. (15). T-CAT consisted of 1 forced and 14 free-choice trials. Consecutive choices made by the mice were counted, and the number of alternations and the percent of alternations different from chance during the 14 free-choice trials were calculated (0%, no alternation; 100%, alternation at each trial; 50%, chance level). The T-maze apparatus, separated from

the investigator by a black curtain, was operated by remote control, and the undisturbed movement of the mice in the maze was observed on a television monitor and videotaped. Statistics were performed using StatView software (SAS Institute, Cary, NC).

The hidden-platform version of the Morris Water Maze (MWM) task (9, 11, 16) was used to assess spatial learning and orientation by LDLR$^{-/-}$ mice on a WD with 300 μg/ml D-4F versus 300 μg/ml of ScD-4F in drinking water. Mice were given a total of 12 training trials (4 trials per day for 3 days), followed by 4 acquisition trails per day for 3 or 4 days, with their performance continuously registered by a video tracking system (SD Instruments, Inc., San Diego, CA). Statistics were performed using StatView software (SAS Institute).

Other procedures

Plasma lipoprotein and lipid levels were determined as described previously (13, 17). Blood pressure was determined by the tail cuff method (18, 19). Electron microscopy was performed as previously described (20).

RESULTS

D-4F decreases hyperlipidemia-induced brain arteriole inflammation

Macrophages (microglia) associated with brain arterioles. Microglia (identified by F4/80 immunostaining) were sparse and were found mainly in the adventitial area of larger brain arterioles (>50 μm) of wild-type and LDLR$^{-/-}$ mice on chow (data not shown). After a WD, even small brain arterioles had associated microglia (**Fig. 1A**), which were located on the adventitial side of the arterioles (Fig. 1B), as previously reported (7, 8). All of the microglia associated with arterioles were on the adventitial side of the vessel, but electron microscopy revealed that many were within the vessel wall as defined as being within the basal lamina. By electron microscopy there were no microglia/macrophages located between the smooth muscle cells and the endothelial cells of the arterioles. The percent of arteri-

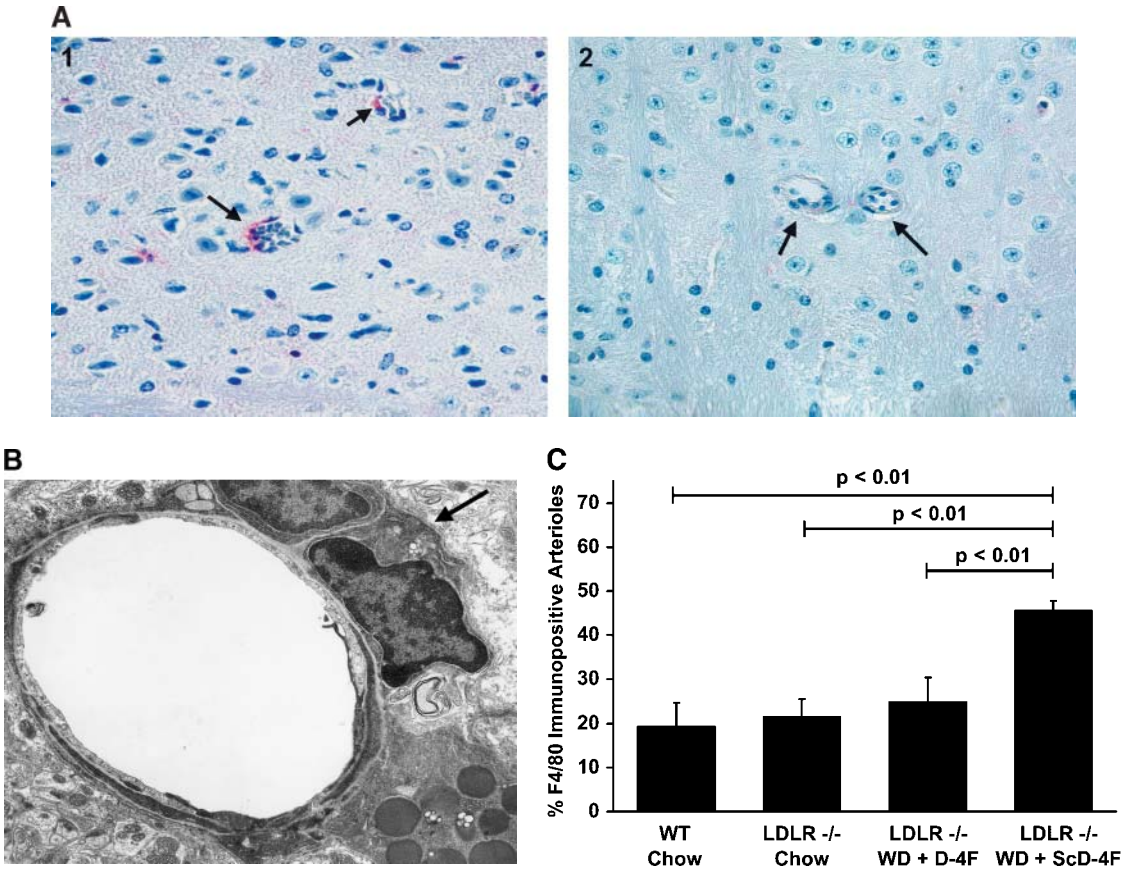

Fig. 1. D-4F, but not scrambled D-4F (ScD-4F), decreases the Western diet (WD)-induced increase in macrophage/microglia associated with brain arterioles in LDR$^{-/-}$ mice. A: F4/80 immunostaining for macrophage/microglia associated with brain arterioles. Shown in panel 1 is an example of brain arterioles (arrows) from an LDLR$^{-/-}$ mouse on a WD with 300 μg/ml of the control inactive peptide ScD-4F in the drinking water (the F4/80 immunostain is red). Shown in panel 2 is an example of brain arterioles (arrows) from an LDLR$^{-/-}$ mouse on a WD with 300 μg/ml D-4F in the drinking water. The magnification for both panels is 200×. Controls treated with secondary antibody only or IgG produced no detectable staining (data not shown). B: An electron microscope image (19,800× magnification) of a brain arteriole with an associated macrophage/microglial cell (arrow) from an LDLR$^{-/-}$ mouse on a WD with 300 μg/ml of the control inactive peptide ScD-4F in the drinking water. C: The percent immunopositive arterioles in 20 microscope fields per brain (examined at 200×) was determined in 8 brains from wild-type mice on chow (WT Chow), 9 brains from LDLR$^{-/-}$ mice on chow (LDLR$^{-/-}$Chow), 9 brains from LDLR$^{-/-}$ mice on the WD with 300 μg/ml D-4F in the drinking water (LDLR$^{-/-}$ WD + D-4F), or in 9 brains from LDLR$^{-/-}$ mice on the WD with 300 μg/ml of the control inactive peptide ScD-4F in the drinking water (LDLR$^{-/-}$ WD + ScD-4F). The data shown are mean ± SEM.

oles immunolabeled by F4/80 antibody more than doubled in LDLR$^{-/-}$ mice on a WD with the control inactive peptide ScD-4F in their drinking water (Fig. 1C). In contrast, the percent of F4/80 immunopositive arterioles on a WD with D-4F in the drinking water was reduced to the levels seen in wild-type and LDLR$^{-/-}$ mice on chow (Fig. 1C). All of the increase in F4/80 immunostaining in the brains of LDLR$^{-/-}$ mice on a WD with the control inactive peptide ScD-4F in the drinking water was associated with arterioles (i.e., there was no increase in F4/80 immunostaining in cells not associated with arterioles) and there was no relationship between nonarteriole-associated F4/80 immunostaining and D-4F treatment (data not shown). There was no significant difference in the number of brain arterioles counted in any treatment group (data not shown).

MIP-1α associated with brain arterioles. The association of MIP-1α with brain arterioles was determined by immunostaining (**Fig. 2A**). The percent of brain arterioles with MIP-1α immunostaining was significantly increased in LDLR$^{-/-}$ mice fed a WD and given the control inactive peptide ScD-4F compared with mice on chow or on a WD with D-4F in their drinking water (Fig. 2B). The distribution of F4/80 immunostaining associated with the brain arterioles was different from that of MIP-1α (Fig. 2C), in that the latter was more broadly distributed, consistent with its role as a secreted chemokine (21) and its known ability to bind to vascular smooth muscle cells (22).

MCP-1 associated with brain arterioles. The association of MCP-1 with brain arterioles was determined by immunostaining (**Fig. 3A, B**). The percent of brain arterioles with associated MCP-1 immunostaining was significantly increased in LDLR$^{-/-}$ mice fed a WD and given the control inactive peptide ScD-4F in their drinking water compared with LDLR$^{-/-}$mice on a chow diet or on a WD with D-4F in their drinking water (Fig. 3C).

D-4F decreases hyperlipidemia-induced brain arteriole wall thickness

Ou et al. (3) reported thickening of the facialis artery in LDLR$^{-/-}$ mice fed a WD that was prevented and reversed by treatment with D-4F. We measured brain arteriole wall thickness in perfusion-fixed brains of wild-type mice and LDLR$^{-/-}$ mice on a chow diet and on a WD. Wall thickness in brain arterioles with a lumen diameter of 15–40 μm was greater in LDLR$^{-/-}$ mice on a chow diet compared with wild-type mice, and was further increased in LDLR$^{-/-}$ mice on a WD (**Fig. 4A**). Similar changes were seen in brain arterioles with lumen diameters of 41–80 μm and 81–160 μm (data not shown). These results suggest that the absence of the LDL receptor significantly increased wall thickness of brain arterioles and that the addition of a WD caused further thickening.

Adding D-4F to the drinking water of LDLR$^{-/-}$ mice on a WD reduced the wall thickness of brain arterioles with a lumen diameter of 21–50 μm compared with the control inactive peptide ScD-4F (Fig. 4B). Similar results were found in brain arterioles with lumen diameters of 10–20 μm and 51–100 μm (data not shown).

To exclude the possibility that dissimilar-sized vessels were compared in the two experimental groups (D-4F versus ScD-4F), which might have accounted for the difference in wall thickness, we measured the internal diameters of all arterioles used for morphometry. There was no significant difference in the lumen size of brain arterioles between the mice receiving D-4F or ScD-4F (Fig. 4C).

Some investigators have suggested that the most reliable measurement of arteriole wall thickness is obtained by dividing the wall thickness for each arteriole by the lumen diameter for that arteriole (23). Figure 4D demonstrates that in 21–50 μm arterioles, the wall-to-lumen ratio was significantly less in mice receiving D-4F compared with the control inactive peptide ScD-4F. Significant reductions were also noted in brain arterioles with lumen diameters of 10–20 μm and 51–100 μm (data not shown).

There was a positive correlation between the number of microglia associated with brain arterioles and the thickness of the wall of the arteriole ($r = 0.6513$ and $r^2 = 0.4241$; $P < 0.0001$). Thus, wall thickness increased in direct proportion to the number of microglia associated with the arterioles. This positive association was not surprising, because as noted above, on electron microscopy, many of the microglia were found incorporated within the basal lamina of the arteriole. However, although highly significant, the correlation suggests that other factors were also involved in causing the increased wall thickness.

D-4F decreases hyperlipidemia-induced brain arteriole smooth muscle α-actin

Perfusion-fixed brains were immunostained for smooth muscle α-actin (**Fig. 5A**). Administration of a WD to LDLR$^{-/-}$ mice resulted in a significant increase in the media-to-lumen ratio as determined from sections immunostained for smooth muscle α-actin (Fig. 5B). In brain arterioles with lumen diameters of 21–50 μm, treatment with D-4F significantly reduced the media-to-lumen ratio compared with mice treated with the control inactive peptide ScD-4F in sections immunostained for smooth muscle α-actin (Fig. 5C). Similar reductions of the media-to-lumen ratio were noted in brain arterioles stained for smooth muscle α-actin with lumen diameters of 10–20 μm and 51–100 μm (data not shown). It was not possible to determine whether the increase in smooth muscle α-actin was due to an increase in smooth muscle cell numbers or increased content of smooth muscle cell α-actin in each smooth muscle cell or some combination of the two. Nor was it possible to quantify how much of the increased wall thickness was due to an increase in extracellular matrix.

D-4F improves hyperlipidemia-induced cognitive impairment

LDLR$^{-/-}$ mice on chow were reported to have impaired cognitive function (24). The mice in our studies were evaluated using two behavioral tests: the T-CAT and the MWM.

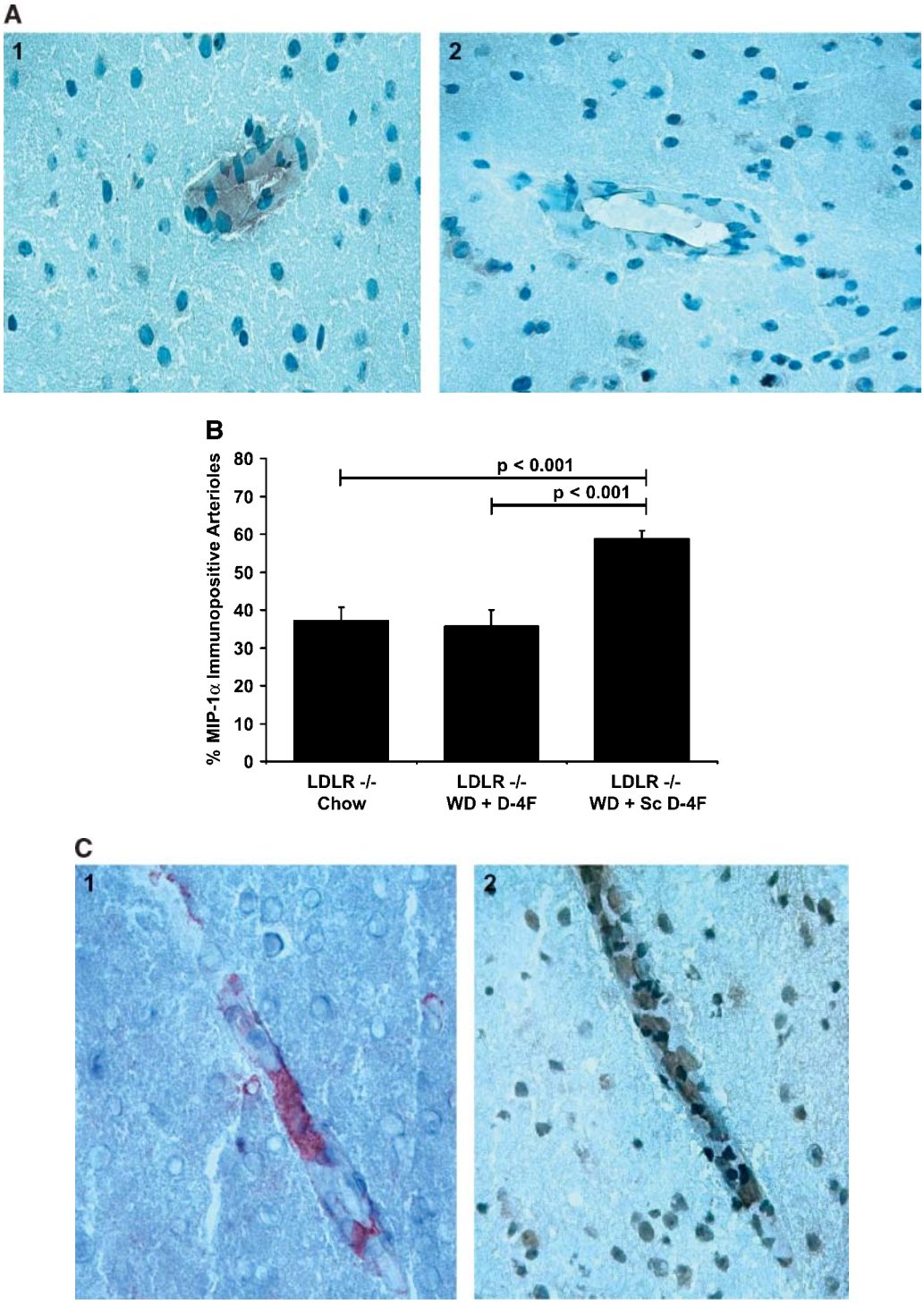

Fig. 2. D-4F, but not ScD-4F, decreases the WD-induced increase in macrophage inflammatory protein-1α (MIP-1α) associated with brain arterioles in LDR$^{-/-}$ mice. A: Shown in panel 1 is an example of a brain arteriole immunostained for MIP-1α in an LDLR$^{-/-}$ mouse on a WD with 300 μg/ml of the control inactive peptide ScD-4F in the drinking water. Shown in panel 2 is an example of a brain arteriole immunostained for MIP-1α in an LDLR$^{-/-}$ mouse on a WD with 300 μg/ml D-4F in the drinking water. Panels 1 and 2 were examined at a magnification of 400×. Control sections treated with secondary antibody alone or with a blocking peptide did not show detectable stain (data not shown). B: The percent immunopositive arterioles in 20 microscope fields per brain (examined at 200×) was determined in 14 brains from LDLR$^{-/-}$ mice on chow (LDLR$^{-/-}$Chow), 14 brains from LDLR$^{-/-}$ mice on the WD with 300 μg/ml D-4F (LDLR$^{-/-}$ WD + D-4F), and in 14 brains from LDLR$^{-/-}$ mice on the WD with 300 μg/ml of the control inactive peptide ScD-4F in the drinking water (LDLR$^{-/-}$ WD + ScD-4F). The data shown are mean ± SEM. C: Serial sections (less than 10 μm apart) containing a longitudinally cut arteriole from an LDLR$^{-/-}$ mouse on the WD with 300 μg/ml of the control inactive peptide ScD-4F in the drinking water were immunostained for F4/80 (panel 1; red-brown stain) and MIP-1α (panel 2; gray-brown stain). Panels 1 and 2 were examined at a magnification of 400×.

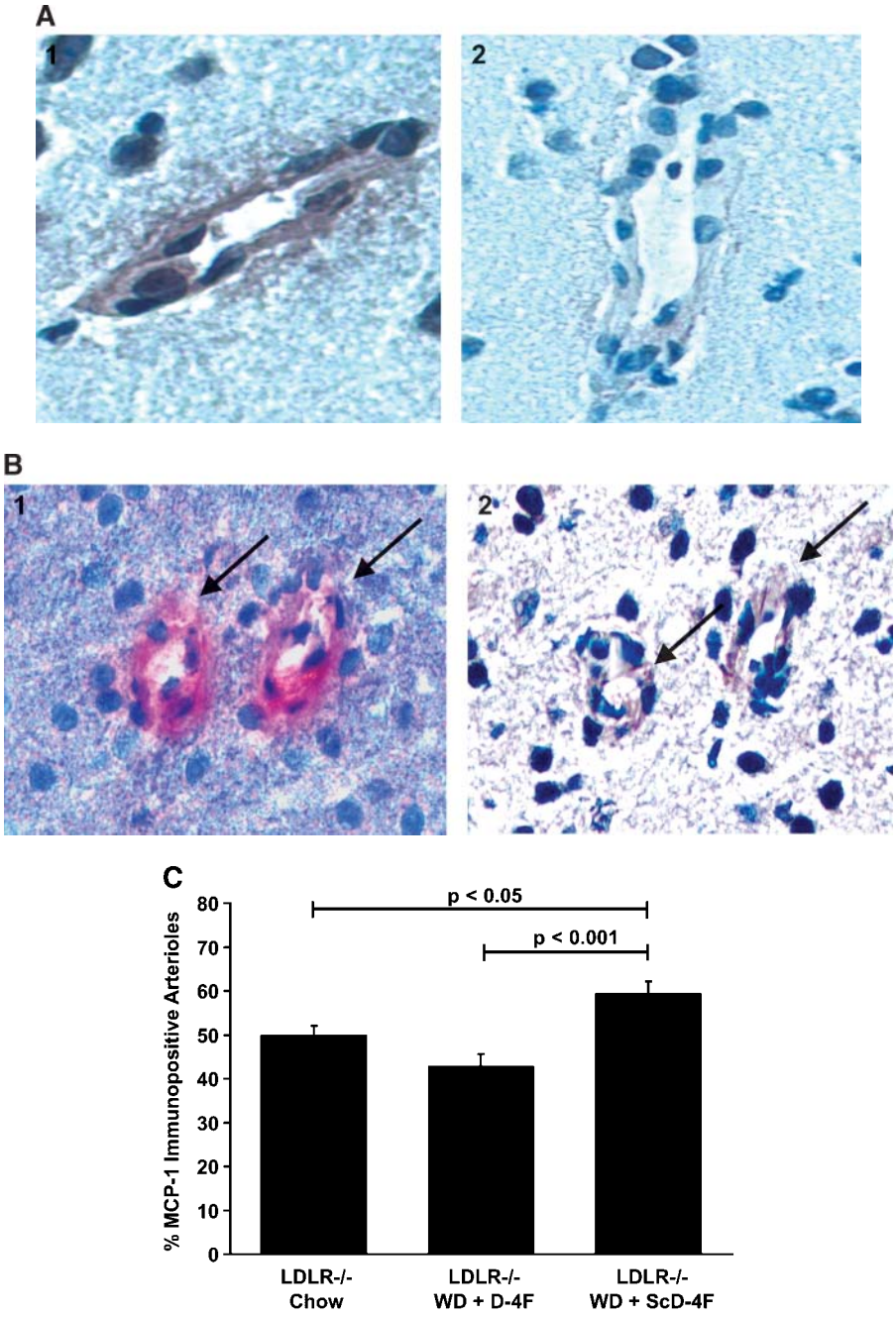

Fig. 3. D-4F, but not ScD-4F, decreases the WD-induced increase in monocyte chemoattractant protein-1 (MCP-1) associated with brain arterioles in LDR$^{-/-}$ mice. A: Shown in panel 1 is an example of a brain arteriole immunostained for MCP-1 in an LDLR$^{-/-}$ mouse on the WD with 300 μg/ml of the control inactive peptide ScD-4F in the drinking water. Shown in panel 2 is an example of a brain arteriole immunostained for MCP-1 in an LDLR$^{-/-}$ mouse on the WD with 300 μg/ml D-4F in the drinking water. Panels 1 and 2 were examined at a magnification of 400×. Control sections were treated with secondary antibody alone or irrelevant IgG and did not show detectable stain (data not shown). B: Serial sections (less than 10 μm apart) from an LDLR$^{-/-}$ mouse on the WD with 300 μg/ml of the control inactive peptide ScD-4F in the drinking water were immunostained for F4/80 (panel 1: arrows; red stain) and MCP-1 (panel 2: arrows, gray-brown stain). C: The percent immunopositive arterioles in 20 microscope fields per brain (examined at 200×) was determined in 15 brains from LDLR$^{-/-}$ mice on chow (LDLR$^{-/-}$Chow), 16 brains from LDLR$^{-/-}$ mice on the WD with 300 μg/ml D-4F in the drinking water (LDLR$^{-/-}$ WD + D-4F), or 15 brains from LDLR$^{-/-}$ mice on the WD with 300 μg/ml of the control inactive peptide ScD-4F in the drinking water (LDLR$^{-/-}$ WD + ScD-4F). The data shown are mean ± SEM.

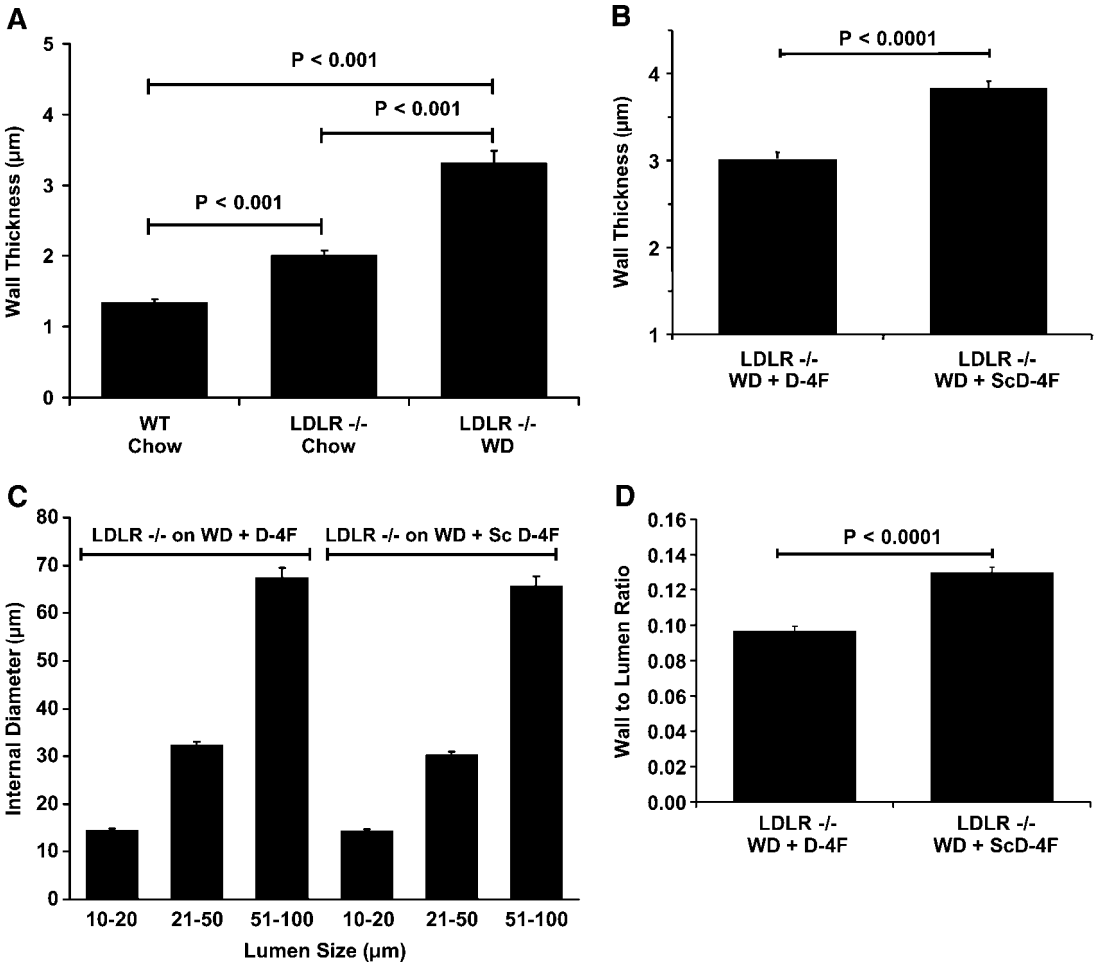

Fig. 4. D-4F, but not ScD-4F, decreases the WD-induced increase in brain arteriole wall thickness in LDR$^{-/-}$ mice. A: Wall thickness (in μm) in H and E-stained brain arterioles (lumen diameter, 15–40 μm) was determined in wild-type mice on chow (WT Chow), LDLR$^{-/-}$ mice on chow (LDLR$^{-/-}$ Chow), or on the WD (LDLR$^{-/-}$ WD). Twenty microscope fields per brain were examined at 400× magnification (n = 4 brains/group). The data shown are mean ± SEM. B: Wall thickness (in μm) in H and E-stained brain arterioles (lumen diameter, 21–50 μm) was determined in LDLR$^{-/-}$ mice on the WD with 300 μg/ml D-4F (LDLR$^{-/-}$ WD + D-4F) or 300 μg/ml of the control inactive peptide ScD-4F in the drinking water (LDLR$^{-/-}$ WD + ScD-4F). Twenty microscope fields per brain were examined at 400× magnification (n = 15 brains/group). The data shown are mean ± SEM. C: H and E-stained brain arterioles from LDLR$^{-/-}$ mice on the WD with 300 μg/ml D-4F or 300 μg/ml of the control inactive peptide ScD-4F in the drinking water were grouped according to lumen diameter. Twenty microscope fields per brain were examined at 400× magnification (n = 15 brains/group). The data shown are mean ± SEM. D: The wall-to-lumen ratio of brain arterioles (lumen diameter, 21–50 μm) was determined in LDLR$^{-/-}$ mice on the WD with 300 μg/ml D-4F (LDLR$^{-/-}$ WD + D-4F) or 300 μg/ml of the control inactive peptide ScD-4F (LDLR$^{-/-}$ WD + ScD-4F) in the drinking water. Twenty microscope fields per brain were examined at 400× magnification (n = 15 brains/group). The data shown are mean ± SEM.

T-CAT. When placed in a T-maze, normal mice will, more often than chance, remember on successive trials that the arm of the T-maze that they entered on the previous trial was a "blind alley" and normal mice will "alternate" on the successive trial to the opposite arm of the T-maze. This process, which involves working memory, is called "spontaneous alternation." In contrast to normal mice, mice with impaired cognition will, more often than chance, enter the blind alley again on the successive trial. Thus, impaired mice will show a significant decrease in the number of spontaneous alternations. There was a significant decrease in the number of alternations in LDLR$^{-/-}$ mice on a WD compared with chow (**Fig. 6A**). On chow, LDLR$^{-/-}$ mice, more often than chance, demonstrated spontaneous alternations, but on a WD, more often than chance, the mice demonstrated impaired behavior (i.e., more often than chance, they returned to the blind alley) (Fig. 6B). Treatment with D-4F (but not the control inactive peptide ScD-4F) improved their working memory, as measured by a significant increase in the number of spontaneous alternations and the percent of alternations different from chance (i.e., different from 50%) (Fig. 6C, D).

MWM. LDLR$^{-/-}$ mice on chow demonstrated a capacity to learn where the underwater platform was located, as indicated by a significant reduction of the daily escape latency, representing the time in seconds necessary to locate and mount the hidden underwater platform (Fig. 6E). On a WD with the control inactive peptide ScD-4F in the drinking water, the mice did not show improvement on successive days (Fig. 6E, F). In contrast, on a WD with D-4F in the drinking water, there was improvement (Fig. 6E, F)

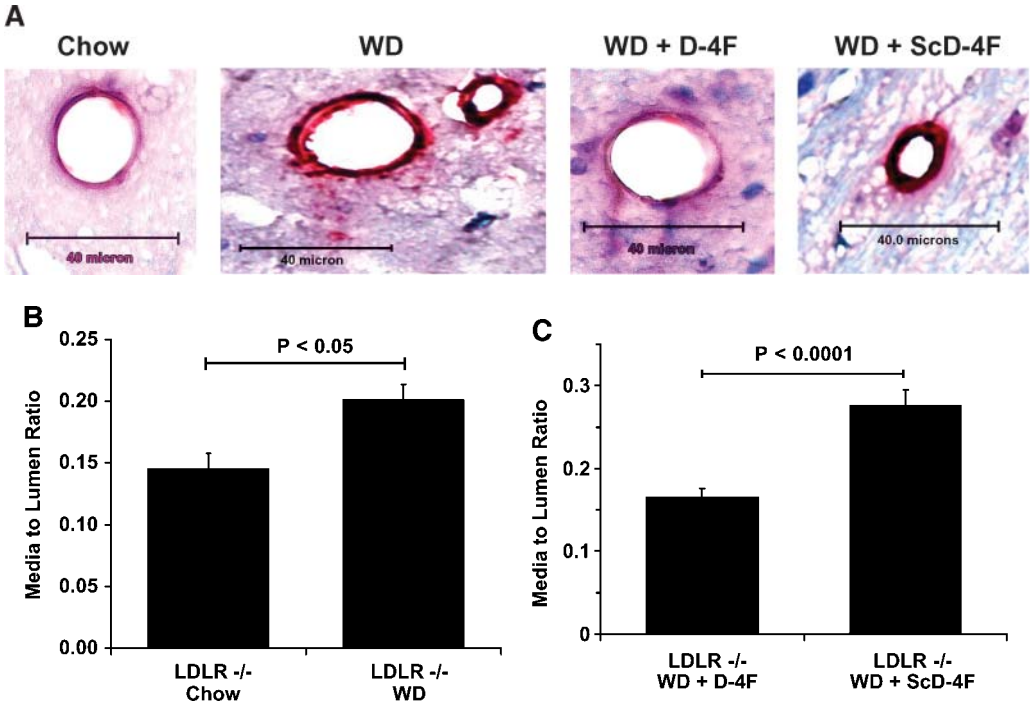

Fig. 5. D-4F, but not ScD-4F, decreases the WD-induced increase in brain arteriole smooth muscle α-actin in $LDR^{-/-}$ mice. A: Examples of smooth muscle α-actin immunostaining in brain arterioles from $LDLR^{-/-}$ mice on chow (Chow), on a WD (WD), on a WD with 300 μg/ml D-4F (WD+ D-4F), or with 300 μg/ml of the control inactive peptide ScD-4F in the drinking water (WD + ScD-4F). B: The media-to-lumen ratio in brain arterioles (lumen diameter, 21–50 μm) was determined in sections stained for smooth muscle cell α-actin from $LDLR^{-/-}$ mice on chow ($LDLR^{-/-}$ Chow) or on a WD ($LDLR^{-/-}$ WD). Twenty microscope fields per brain were examined at 400× magnification (n = 10 brains/group). The data shown are mean ± SEM. C: The media-to-lumen ratio of brain arterioles (lumen diameter, 21–50 μm) was determined in sections stained for smooth muscle cell α-actin in $LDLR^{-/-}$ mice on the WD with 300 μg/ml D-4F ($LDLR^{-/-}$ WD + D-4F) or 300 μg/ml of the control inactive peptide ScD-4F in the drinking water ($LDLR^{-/-}$ WD + ScD-4F). Twenty microscope fields per brain were examined at 400× magnification (n = 15 brains/group). The data shown are mean ± SEM.

to the level of performance seen in $LDLR^{-/-}$ mice on chow (Fig. 6E).

D-4F did not alter blood pressure or plasma lipids

Trieu and Uckun (19) reported that feeding a WD to male (but not female) $LDLR^{-/-}$ mice resulted in increased blood pressure. Because our mice were female, we would not have expected the WD to alter their blood pressure. Indeed, this was the case, and D-4F also did not alter blood pressure (data not shown).

There was no significant difference in the concentrations of plasma total cholesterol, LDL+VLDL-cholesterol, HDL-cholesterol, or triglycerides when the mice were administered D-4F compared with the control inactive peptide ScD-4F (**Table 1**).

D-4F reduces MCP-1 and MIP-1α expression in nonvascular brain cells

Because D-4F improved performance in the T-CAT and MWM tests without altering plasma lipids, blood pressure, or arteriole lumen diameter in brains fixed at physiologic perfusion pressures, we considered the possibility that chemokines induced in brain arterioles by the WD may have spread to adjacent nonvascular brain cells. Perhaps soluble chemokines such as MCP-1 and MIP-1α, which were produced by the arterioles in response to the WD (Figs. 2, 3), may have acted on adjacent nonvascular brain cells. Chemokines have been shown to be synthesized by all major cell types in the brain, i.e., neurons, glia, microglia, and all major cell types in the brain have the receptors for these chemokines (25, 26). Therefore, we determined the percent of nonvascular cells immunopositive for MCP-1 and MIP-1α within 150 μm surrounding each brain arteriole (**Fig. 7**). The percent of nonvascular cells that were immunopositive for MCP-1 (Fig. 7A, B) and MIP-1α (Fig. 7C) in $LDLR^{-/-}$ mice on a WD with the control inactive peptide ScD-4F in the drinking water was significantly greater compared with mice on chow or on a WD with D-4F in the drinking water. The total number of nonvascular cells in the area surrounding each brain arteriole was not different between groups (data not shown).

DISCUSSION

The data presented here demonstrate for the first time that hyperlipidemia induces inflammation of vessels as small as arterioles. The inflammatory response is similar to

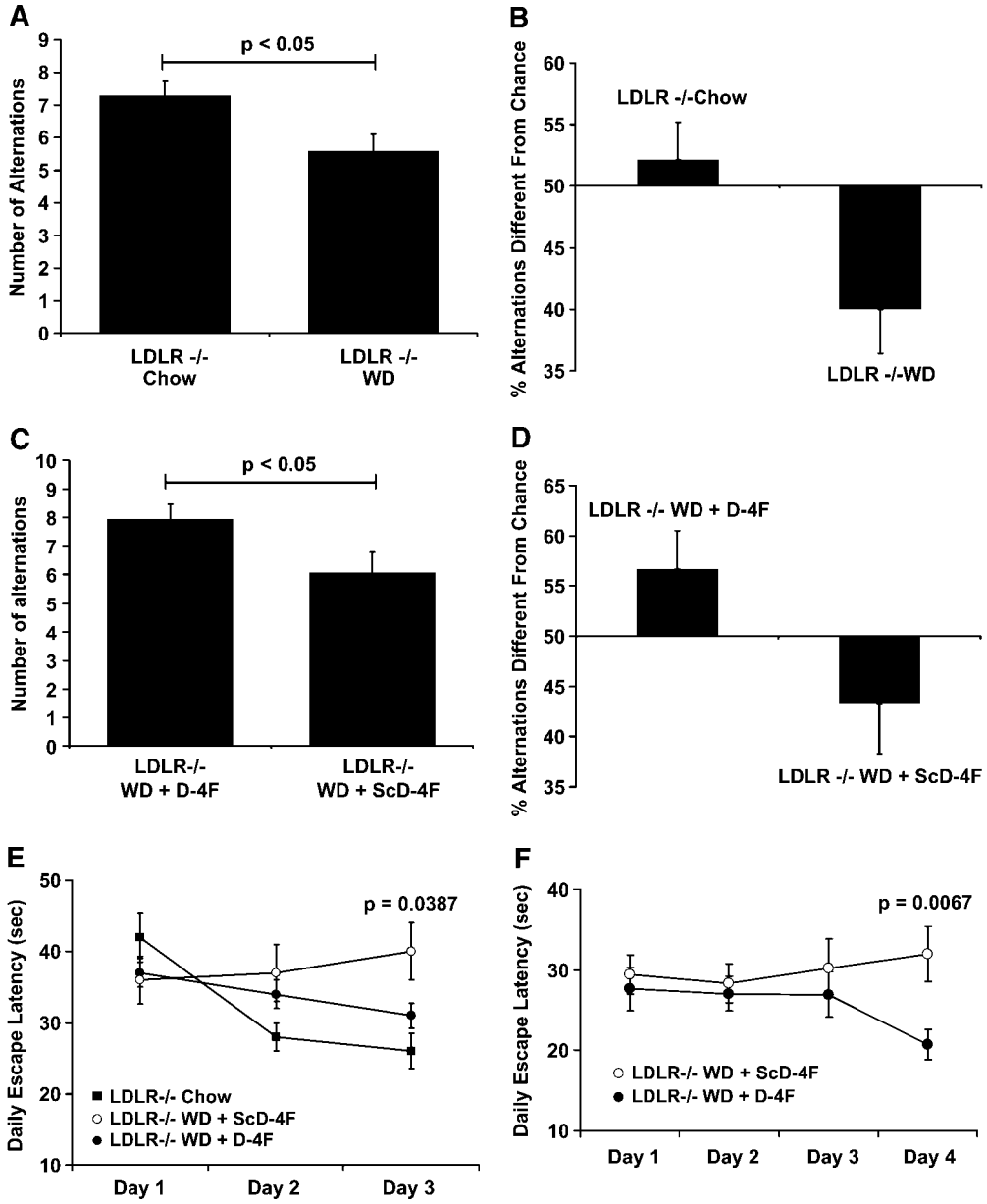

Fig. 6. D-4F, but not ScD-4F, ameliorates WD-induced impairment in cognitive function in $LDR^{-/-}$ mice. A–D: The performance of $LDLR^{-/-}$ mice in the T-maze continuous alternation task (T-CAT) was determined as described in Materials and Methods. A: The number of spontaneous alternations on the WD versus chow was determined. The data shown are mean ± SEM of 10 mice in each group tested in 14 free-choice trials, as described in Materials and Methods. B: The percent alternations different from chance (0%, no alternation; 100%, alternation at each trial; 50%, chance level) for mice described in A. The data shown are mean ± SEM of 10 mice in each group tested in 14 free-choice trials, as described in Materials and Methods. C: The number of spontaneous alternations was determined in $LDLR^{-/-}$ mice on the WD with 300 μg/ml D-4F ($LDLR^{-/-}$ WD + D-4F) or 300 μg/ml of the control inactive peptide ScD-4F in the drinking water ($LDLR^{-/-}$ WD + ScD-4F). The data shown are mean ± SEM of 15 mice in each group tested in 14 free-choice trials, as described in Materials and Methods. D: The percent alternations different from chance (0%, no alternation; 100%, alternation at each trial; 50%, chance level) for mice described in C. The data shown are mean ± SEM of 15 mice in each group tested in 14 free-choice trials, as described in Materials and Methods. E and F: The performance of $LDLR^{-/-}$ mice in the Morris Water Maze was determined. E: The time in seconds required to locate and climb onto the hidden underwater platform (daily escape latency) was determined in $LDLR^{-/-}$ mice on chow ($LDR^{-/-}$ Chow; closed squares) versus $LDLR^{-/-}$ mice on the WD with 300 μg/ml of the control inactive peptide ScD-4F ($LDLR^{-/-}$ WD + ScD-4F; open circles) versus $LDLR^{-/-}$ mice on the WD with 300 μg/ml D-4F in the drinking water ($LDLR^{-/-}$ WD + D-4F; closed circles). The data shown are mean ± SEM from four acquisition trials/day/mouse for three consecutive days, with 16 mice in each group, with tests for statistical significance by repeated-measures ANOVA ($P = 0.0387$). F: A repeat study was performed with another group of $LDLR^{-/-}$ mice on the WD with 300 μg/ml of the control inactive peptide ScD-4F ($LDLR^{-/-}$ WD + ScD-4F; open circles) in the drinking water versus 300 μg/ml D-4F in the drinking water ($LDLR^{-/-}$ WD + D-4F; closed circles). The data shown are mean ± SEM from four acquisition trials/day/mouse for four consecutive days with 15 mice in each group, with tests for statistical significance by repeated-measures ANOVA ($P = 0.0067$).

TABLE 1. Plasma lipid and lipoprotein levels in LDLR$^{-/-}$ mice fed a Western diet (WD)

	D-4F	ScD-4F
	mg/dl	
Total cholesterol	1,076 ± 75	970 ± 61
LDL+VLDL-cholesterol	924 ± 76	834 ± 63
HDL-cholesterol	86 ± 6	79 ± 5
Triglycerides	330 ± 25	288 ± 25

LDLR$^{-/-}$ mice were fed a WD as described in Materials and Methods and received D-4F or the control inactive peptide ScD-4F in their drinking water at a concentration of 300 μg/ml. The values shown are the mean ± SD.

that induced in larger vessels, in that the components include macrophage-like cells and chemokines associated with a macrophage-mediated inflammatory response (MIP-1α and MCP-1). However, the location of the microglia was quite different in brain arterioles compared with the location of macrophage cells in larger arterial vessels. The microglia were always located on the adventitial side of the arteriole, never between the smooth muscle cells and the endothelial cells. Often the microglia were incorporated within the basal lamina of the arteriole, indicating the intimate nature of the association.

The positive correlation between the number of microglia per arteriole and wall thickness indicates that the number of microglia per arteriole directly contributed to wall thickness (i.e., the incorporation of some microglia within the basal lamina of the arteriole wall directly contributed to the measurements of wall thickness as measured in H and E-stained sections). However, the correlation ($r^2 = 0.4241$; $P < 0.0001$), although highly significant, also suggests that other factors must have been involved in determining wall thickness differences between the treatment groups. Wall thickness increases with increasing vessel size (measured by the internal diameter of the vessel), and so it is critical to compare vessels of comparable size. Therefore, all of our studies compared vessels of similar size from the different treatment groups, as stated in the text and as illustrated by the data in Fig. 4C.

Bush et al. (27) have emphasized the importance of monocyte-macrophages and MCP-1 in vascular hypertrophy. Perhaps the microglia associated with brain arterioles in LDLR$^{-/-}$ mice on a WD also indirectly contributed to the increase in brain arteriole smooth muscle α-actin via the secretion of MCP-1.

We chose to study the two CC (β-chemokine) family members CCL2/MCP-1 and CCL3/MIP-1α because they are both frequently secreted during wound healing and following neurotrauma. For example, after target ablation by olfactory bulbectomy, there was synchronized degenerative cell death of olfactory neurons followed by infiltration of macrophages that was mediated by MIP-1α and MCP-1 (28). After deletion of mitogen-activated protein kinase-activated protein kinase 2 in mice, the release of both of these chemokines was inhibited from bacterial lipopolysaccharide and interferon-γ-stimulated microglial cells (21). MCP-1 is secreted by cytokine-stimulated vascular smooth muscle cells (29), as is the case for cytokine-stimulated endothelial cells (30). Additionally, MIP-1α and MCP-1 are both found in lesions of mouse models of atherosclerosis (31).

The LDL-mediated induction of chemokines by human artery wall cells is mediated by oxidized lipids that are removed or inactivated by apoA-I, normal HDL, and the antioxidant enzyme associated with HDL, paraoxonase (32, 33). In addition to contributing to LDL induction of chemokine production by artery wall cells, these oxidized lipids inhibit some of the antioxidant enzymes associated with HDL (34). D-4F is an apoA-I mimetic peptide that removes these oxidized lipids from lipoproteins (34). As a result of the removal of these oxidized lipids, the antioxidant enzymes associated with HDL are activated and there is a further reduction in the proinflammatory lipids (34). As a result, D-4F significantly reduces lesions in mouse models of atherosclerosis (35) and reduces inflammation after viral infection (36, 37). Although we did not measure these parameters in this study, these properties of D-4F presumably contributed to the beneficial effects demonstrated here.

The increase in the percent of brain arterioles with associated macrophages (Fig. 1) was approximately 2-fold on the WD. Although the increases in MIP-1α (Fig. 2) and MCP-1 (Fig. 3) were highly significant, they were less than 2-fold. This discrepancy may suggest that other as yet unidentified chemokines may play an important role in hyperlipidemia-induced arteriole inflammation.

We chose to use only female mice in these studies because of their relative behavioral placidity and because they have previously been found to be immune from the increase in blood pressure that follows feeding the WD to male LDLR$^{-/-}$ mice (19). Our results confirmed those of Trieu and Uckun (19) in that we did not find any change in blood pressure with administration of the WD in these female mice, nor did we see a change in blood pressure with administration of either D-4F or the inactive control peptide ScD-4F.

The results presented here, together with those previously reported (1–3), indicate that a WD in LDLR$^{-/-}$ mice induces an inflammatory response throughout the arterial tree. In arterioles, the macrophages are located on the adventitial side of the vessel (7, 8) in close proximity to nonvascular cells. As reported here, by electron microscopy, many of the microglia were incorporated into the wall of the arteriole within the basal lamina. Because apoB-containing lipoproteins do not cross the blood-brain barrier, the improvement of cognitive behavior in the T-CAT and MWM tests (Fig. 6) after D-4F treatment may be due, at least in part, to the reduction in the inflammatory response (as assessed by MIP-1α and MCP-1 immunostaining) of nonvascular cells adjacent to brain arterioles in the D-4F-treated mice (Fig. 7). Chemokines are produced by all major cell types in the brain, and the major cell types in the brain have the receptors for these chemokines, suggesting that chemokine signaling in the brain probably has functions beyond a role in neuroinflammation (e.g., chemokine receptors expressed by mature neurons may regulate synaptic transmission and neuronal survival) (25, 26).

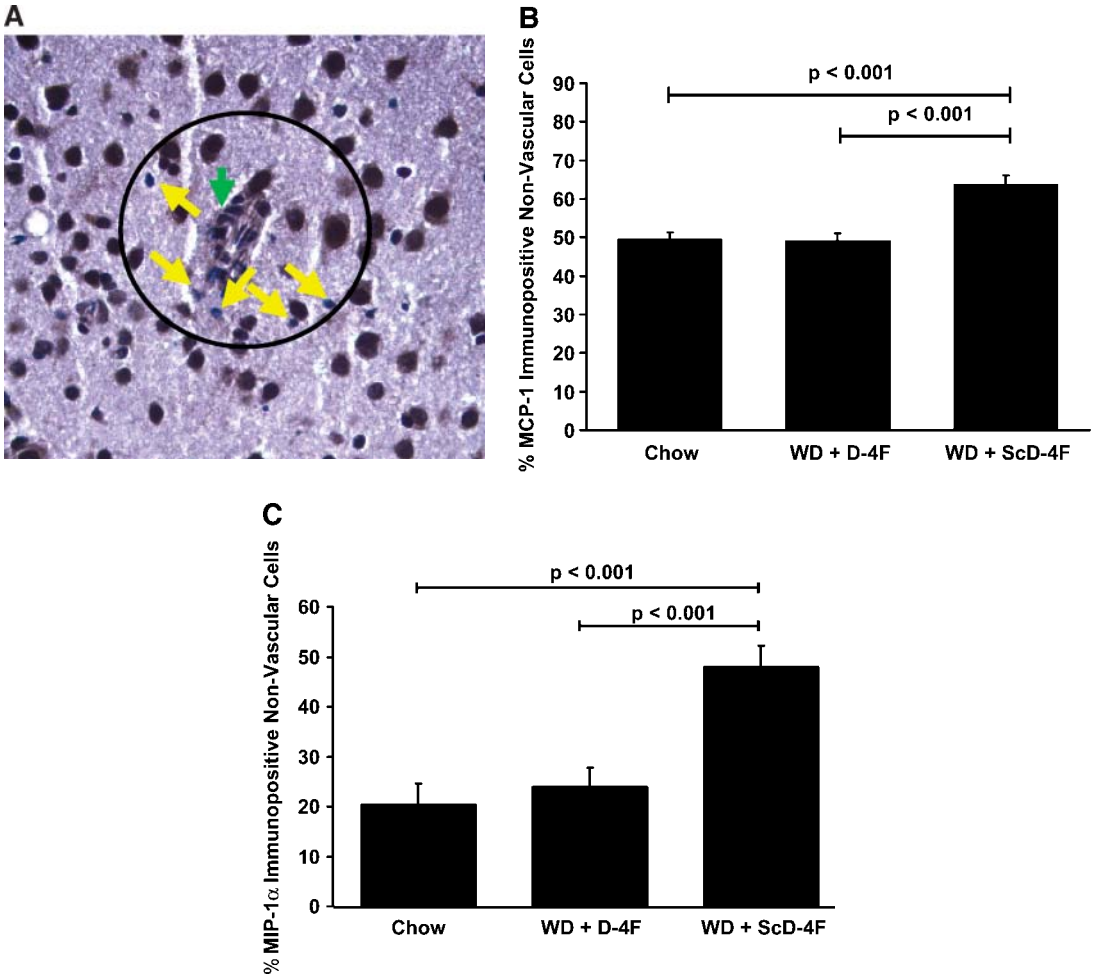

Fig. 7. D-4F, but not ScD-4F, decreases the WD-induced increase in MCP-1 and MIP-1α immunostaining of nonvascular brain cells. A: An example of an MCP-1 immunostained brain section from LDLR$^{-/-}$ mouse on the WD with 300 μg/ml of the control inactive peptide ScD-4F in the drinking water. The black line defines a circle with a diameter of 150 μm with a brain arteriole in the center (green arrow). The yellow arrows point to five nonarteriole cells that did not stain positively for MCP-1. All of the other cells within the circle have stained positively for MCP-1. B: A circle with a diameter of 150 μm was drawn around each brain arteriole in 20 photographed sections immunostained for MCP-1 from each brain taken from 15 LDLR$^{-/-}$ mice on a chow diet (Chow), 16 LDLR$^{-/-}$ mice on a WD with 300 μg/ml D-4F (WD + D-4F), or 15 LDLR$^{-/-}$ mice on a WD with 300 μg/ml of the control inactive peptide ScD-4F in the drinking water (WD + ScD-4F). The percent of nonvascular cells within the circle around the brain arterioles that immunostained for MCP-1 was determined. The data shown are mean ± SEM. C: A circle with a diameter of 150 μm was drawn around each brain arteriole in 20 photographed sections immunostained for MIP-1α from each brain taken from 6 LDLR$^{-/-}$ mice on a chow diet (Chow), 6 LDLR$^{-/-}$ mice on a WD with 300 μg/ml D-4F (WD + D-4F), or 6 LDLR$^{-/-}$ mice on a WD with 300 μg/ml of the control inactive peptide ScD-4F in the drinking water (WD + ScD-4F). The percent of nonvascular cells within the circle around the brain arterioles that immunostained for MIP-1α was determined. The data shown are mean ± SEM.

It has long been assumed that tissue dysfunction induced by hyperlipidemia in the absence of obstruction of the vascular lumen was due to abnormalities in vascular reactivity that may alter blood flow to the tissues. We did not measure cerebral blood flow in the current studies. It is entirely possible that alterations in cerebral blood flow due to alterations in vasoreactivity may have contributed to the observed changes in cognitive function. However, the data presented here suggest that such changes may also be due, in part, to the spread of chemokines from brain arterioles to adjacent nonvascular brain cells (Fig. 7). The data presented here, although consistent with this hypothesis, do not conclusively establish that the changes in cognitive function were due to inflammatory chemokines radiating from brain arterioles. It is possible that the WD induced a generalized inflammation of the brain that was independent of arteriole inflammation. For example, it may be that a generalized increase in circulating cytokines was induced by the WD and that these cytokines acted on the brain cells directly. We did not measure circulating cytokines in these studies. D-4F is known to be associated with HDL (34), and we do not know whether D-4F crosses the blood-brain barrier. We do know that D-4F can reduce the levels of circulating cytokines (36), and this action appears to be related to its ability to reduce proinflammatory oxidized lipids (37).

Speaking against the possibility that the WD induced a generalized inflammation of the brain that was mitigated

by D-4F was the finding that upon feeding the WD, F4/80 immunostaining only increased in association with arterioles. Moreover, F4/80 immunostaining was only reduced by D-4F in this location. Upon feeding the WD, there was no increase in F4/80 immunostaining of the brain that was not intimately associated with the arterioles. Moreover, F4/80 immunostaining of the brain in areas removed from the arterioles was not affected by any of the treatments. Therefore, we believe that the concept of arterioles as centers of hyperlipidemia-induced inflammation from which soluble chemokines can spread to adjacent nonvascular cells and induce dysfunction is novel and deserving of further study.

The ability of oral D-4F to decrease the WD-induced inflammation associated with brain arterioles and the ability of D-4F to ameliorate the WD-induced deterioration in cognitive performance without altering blood pressure, plasma lipid, or lipoprotein levels suggests that apoA-I and apoA-I mimetic peptides may have therapeutic potential in a variety of diseases of small arterial vessels.

This work was supported in part by US Public Health Service Grants HL-30568 (A.M.F.) and HL-34343 (G.M.A.) and the Laubisch, Castera, and M. K. Grey Funds (A.M.F.) at the University of California–Los Angeles. The authors are thankful to Dr. Kenneth Roos for guidance and help with the blood pressure measurements and to University of California–Los Angeles students Anthony Dao, Chi Tran, and Lac Tran for their valuable help with photomicrography, morphometry, and graphics.

REFERENCES

1. Breslow, J. L. 1996. Mouse models of atherosclerosis. *Science.* **272:** 685–688.
2. Schiller, N. K., A. S. Black, G. P. Bradshaw, D. J. Bonnet, and L. K. Curtiss. 2004. Participation of macrophages in atherosclerotic lesion morphology in LDLr$^{-/-}$ mice. *J. Lipid Res.* **45:** 1398–1409.
3. Ou, J., J. Wang, H. Xu, Z. Ou, M. G. Sorci-Thomas, D. W. Jones, P. Signorino, J. C. Densmore, S. Kaul, K. T. Oldham, et al. 2005. Effects of D-4F on vasodilation and vessel wall thickness in hypercholesterolemic LDL receptor-null and LDL receptor/apolipoprotein A-I double-knockout mice on Western diet. *Circ. Res.* **97:** 1190–1197.
4. Joris, I., E. Stetz, and G. Majno. 1979. Lymphocytes and monocytes in the aortic intima—An electron microscopic study in the rat. *Atherosclerosis.* **34:** 221–231.
5. Napoli, C., F. P. D'Armiento, F. P. Macini, A. Postiglione, J. L. Witztum, G. Palumbo, and W. Palinski. 1997. Fatty streak formation occurs in human fetal aorta and is greatly enhanced by maternal hypercholesterolemia. Intimal accumulation of low density lipoprotein and its oxidation precede monocyte recruitment into early atherosclerotic lesions. *J. Clin. Invest.* **100:** 2680–2690.
6. Navab, M., J. A. Berliner, G. Subbanagounder, S. Hama, A. J. Lusis, L. W. Castellani, S. Reddy, D. Shih, W. Shi, A. D. Watson, et al. 2001. HDL and the inflammatory response induced by LDL-derived oxidized phospholipids. *Arterioscler. Thromb. Vasc. Biol.* **21:** 481–488.
7. Mato, M., S. Ookawara, A. Sakamoto, E. Aikawa, T. Ogawa, U. Mitsuhashi, T. Masuzawa, H. Suzuki, M. Honda, Y. Yazaki, et al. 1996. Involvement of specific macrophage-lineage cells surrounding arterioles in barrier and scavenger function in brain cortex. *Proc. Natl. Acad. Sci. USA.* **93:** 3269–3274.
8. Mato, M., S. Ookawara, T. Mashiko, A. Sakamoto, T. K. Mato, N. Maeda, and T. Kodama. 1999. Regional difference of lipid distribution in brain of apolipoprotein E deficient mice. *Anat. Rec.* **256:** 165–176.
9. Li, L., D. Cao, D. W. Garber, H. Kim, and K. Fukuchi. 2003. Association of aortic atherosclerosis with cerebral beta-amyloidosis and learning deficits in a mouse model of Alzheimer's disease. *Am. J. Pathol.* **163:** 2155–2164.
10. Kunjathoor, V. V., A. A. Tseng, L. A. Medeiros, T. Khan, and K. J. Moore. 2004. β-Amyloid promotes accumulation of lipid peroxides by inhibiting CD36-mediated clearance of oxidized lipoproteins. *J Neuroinflammation.* **1:** 23–35.
11. Cao, D., K. I. Fukuchi, H. Wan, H. Kim, and L. Li. 2005. Lack of LDL receptor aggravates learning deficits and amyloid deposits in Alzheimer transgenic mice. *Neurobiol Aging.* Epub ahead of print. October 14, 2005; doi:10.1016/j.neurobiolaging.2005.09.011.
12. Grammas, P., and R. Ovase. 2001. Inflammatory factors are elevated in brain microvessels in Alzheimer's disease. *Neurobiol. Aging.* **22:** 837–842.
13. Navab, M., G. M. Anantharamaiah, S. T. Reddy, S. Hama, G. Hough, V. R. Grijalva, A. C. Wagner, J. S. Frank, G. Datta, D. Garber, et al. 2004. Oral D-4F causes formation of pre-β high-density lipoprotein and improves high-density lipoprotein-mediated cholesterol efflux and reverse cholesterol transport from macrophages in apolipoprotein E-null mice. *Circulation.* **109:** 3215–3220.
14. Fernagut, P. O., E. Diguet, N. Stefanova, M. Biran, G. K. Wenning, P. Canioni, B. Bioulac, and F. Tison. 2002. Subacute systemic 3-nitropropionic acid intoxication induces a distinct motor disorder in adult C57BL/6 mice: behavioural and histopathological characterization. *Neuroscience.* **114:** 1005–1017.
15. Gerlai, R. 1998. A new continuous alternation task in T-maze detects hippocampal dysfunction in mice. A strain comparison and lesion study. *Behav. Brain Res.* **95:** 91–101.
16. Costa, R. M., N. B. Federov, J. H. Kogan, G. G. Murphy, J. Stern, M. Ohno, R. Kucherlapati, T. Jacks, and A. J. Silva. 2002. Mechanism for the learning deficits in a mouse model of neurofibromatosis type 1. *Nature.* **415:** 526–530.
17. Navab, M., G. M. Anantharamaiah, S. Hama, G. Hough, S. T. Reddy, J. S. Frank, D. W. Garber, S. Handattu, and A. M. Fogelman. 2005. D-4F and statins synergize to render HDL anti-inflammatory in mice and monkeys and cause lesion regression in old apolipoprotein E-null mice. *Arterioscler. Thromb. Vasc. Biol.* **25:** 1426–1432.
18. Manning, M. W., L. A. Cassis, and A. Daugherty. 2003. Differential effects of doxycycline, a broad-spectrum matrix metalloproteinase inhibitor, on angiotensin II-induced atherosclerosis and abdominal aortic aneurysms. *Arterioscler. Thromb. Vasc. Biol.* **23:** 483–488.
19. Trieu, V. N., and F. M. Uckun. 1998. Male-associated hypertension in LDL-R deficient mice. *Biochem. Biophys. Res. Commun.* **247:** 277–279.
20. Dansky, H. M., S. A. Charlton, C. B. Barlow, M. Tamminen, J. D. Smith, J. S. Frank, and J. L. Breslow. 1999. Apo A-I inhibits foam cell formation in apo E-deficient mice after monocyte adherence to endothelium. *J. Clin. Invest.* **104:** 31–39.
21. Culbert, A. A., S. D. Skaper, D. R. Howlett, N. A. Evans, L. Facci, P. E. Soden, Z. M. Seymour, F. Guillot, M. Gaestel, and J. C. Richardson. 2006. MAPKAP kinase 2 deficiency in microglia inhibits pro-inflammatory mediator release and resultant neurotoxicity: Relevance to neuroinflammation in a transgenic mouse model of Alzheimer's disease. *J. Biol. Chem.* Epub ahead of print. June 14, 2006; doi:10.1074/jbc.M513646200.
22. Hayes, I. M., N. J. Jordan, S. Towers, G. Smith, J. R. Paterson, J. J. Earnshaw, A. G. Roach, J. Westwick, and R. J. Williams. 1998. Human vascular smooth muscle cells express receptors for CC chemokines. *Arterioscler. Thromb. Vasc. Biol.* **18:** 397–403.
23. Mulvany, M. J. 2002. Small artery remodeling and significance in the development of hypertension. *News Physiol. Sci.* **17:** 105–109.
24. Mulder, M., P. J. Jansen, B. J. A. Janssen, W. D. J. van de Berg, H. van der Boom, L. M. Havekes, R. E. de Kloet, F. C. S. Ramaekers, and A. Blokland. 2004. Low-density lipoprotein receptor-knockout mice display impaired spatial memory associated with a decreased synaptic density in the hippocampus. *Neurobiol. Dis.* **16:** 212–219.
25. Bajetto, A., R. Bonavia, S. Barbero, and G. Schettini. 2002. Characterization of chemokines and their receptors in the central nervous system: physiological implications. *J. Neurochem.* **82:** 1311–1329.
26. Tran, P. B., D. Ren, T. J. Veldhouse, and R. J. Miller. 2004. Chemokine receptors are expressed widely by embryonic and adult neural progenitor cells. *J. Neurosci. Res.* **76:** 20–34.
27. Bush, E., N. Maeda, W. A. Kuziel, T. C. Dawson, J. N. Wilcox, H. DeLeon, and W. R. Taylor. 2000. CC chemokine receptor 2 is required for macrophage infiltration and vascular hypertrophy in angiotensin II-induced hypertension. *Hypertension.* **36:** 360–363.

28. Getchell, T. V., N. K. Subhedar, D. S. Shah, G. Hackley, J. V. Partin, G. Sen, and M. L. Getchell. 2002. Chemokine regulation of macrophage recruitment into the olfactory epithelium following target ablation: involvement of macrophage inflammatory protein-1α and monocyte chemoattractant protein-1. *J. Neurosci. Res.* **70:** 784–793.
29. Schaub, F. J., W. C. Liles, N. Ferri, K. Sayson, R. A. Seifert, and D. F. Bowen-Pope. 2003. Fas and fas-associated death domain protein regulate monocyte chemoattractant protein-1 expression by human smooth muscle cells through caspase- and calpain-dependent release of interleukin-1α. *Circ. Res.* **93:** 515–522.
30. Volk, T., M. Hensel, H. Schuster, and W. J. Kox. 2000. Secretion of MCP-1 and IL-6 by cytokine stimulated production of reactive oxygen species in endothelial cells. *Mol. Cell. Biochem.* **206:** 105–112.
31. Dol, F., G. Martin, B. Staels, A-M. Mares, C. Cazaubon, D. Nisato, J-P. Bidouard, P. Janiak, P. Schaeffer, and J-M. Herbert. 2001. Angiotensin AT1 receptor antagonist irbesartan decreases lesion size, chemokine expression, and macrophage accumulation in apolipoprotein E-deficient mice. *J. Cardiovasc. Pharmacol.* **38:** 395–405.
32. Navab, M., S. Y. Hama, C. J. Cooke, G. M. Anantharamaiah, M. Chaddha, L. Jin, G. Subbanagounder, K. F. Faull, S. T. Reddy, N. E. Miller, et al. 2000. Normal high density lipoprotein inhibits three steps in the formation of mildly oxidized low density lipoprotein: step 1. *J. Lipid Res.* **41:** 1481–1494.
33. Navab, M., S. Y. Hama, G. M. Anantharamaiah, K. Hassan, G. P. Hough, A. D. Watson, S. T. Reddy, A. Sevanian, G. C. Fonarow, and A. M. Fogelman. 2000. Normal high density lipoprotein inhibits three steps in the formation of mildly oxidized low density lipoprotein: steps 2 and 3. *J. Lipid Res.* **41:** 1495–1508.
34. Navab, M., G. M. Anantharamaiah, S. T. Reddy, S. Hama, G. Hough, V. R. Grijalva, N. Yu, B. J. Ansell, G. Datta, D. W. Garber, et al. 2005. Apolipoprotein A-I mimetic peptides. *Arterioscler. Thromb. Vasc. Biol.* **25:** 1325–1331.
35. Navab, M., G. M. Anantharamaiah, S. Hama, D. W. Garber, M. Chaddha, G. Hough, R. Lallone, and A. M. Fogelman. 2002. Oral administration of an apo A-I mimetic peptide synthesized from D-amino acids dramatically reduces atherosclerosis in mice independent of plasma cholesterol. *Circulation.* **105:** 290–292.
36. Van Lenten, B. J., A. C. Wagner, G. M. Anantharamaiah, D. W. Garber, M. C. Fishbein, L. Adhikary, D. P. Nayak, S. Hama, M. Navab, and A. M. Fogelman. 2002. Influenza infection promotes macrophage traffic into arteries of mice that is prevented by D-4F, an apolipoprotein A-I mimetic peptide. *Circulation.* **106:** 1127–1132.
37. Van Lenten, B. J., A. C. Wagner, M. Navab, G. M. Anantharamaiah, E. K-W. Hui, D. P. Nayak, and A. M. Fogelman. 2004. D-4F, an apolipoprotein A-I mimetic peptide, inhibits the inflammatory response induced by influenza A infection of human type II pneumocytes. *Circulation.* **110:** 3252–3258.